We are grateful to the Reviewer 2 for reviewing our article and for the very useful comments that allowed us to improve this manuscript. Below are our responses to the Reviewer's comments.

line 100: Is it correct that all cameras were recovered undamaged and fully functional? So why did two of three not provide data? Was it a software/datastorage/telemetry issue? Investigating the problem might inform future missions.
Yes, it is correct that all cameras were recovered undamaged and fully functional. As we pointed out in lines 100-103, two of three cameras (wide-angle and narrow-angle) functioned for the first 13 h and 12 h, respectively, before ceasing operation for unknown reasons. The data from these two cameras are available but have not been analyzed in detail so far. We preliminary checked the data from these cameras that confirm registration of NLC both on large and small scales in the beginning of the TRANSAT flight.

We don't really know what happened to these two cameras after 12 hours of the flight in the stratosphere. There is no telemetry about the internal state of the cameras. It should be noted that all three cameras had already been in the stratosphere for about 13 hours at low temperatures of -30°C and were functioning normally (Dalin et al., 2022). Taking into account the previous positive balloon-borne experiment, it was decided to use all three cameras for the long-duration TRANSAT flight in the stratosphere.

At the same time, it should be noted that these SONY cameras are commercial cameras that are not designed for a flight in the stratosphere in 24/7 sunlight, at low temperatures and lack of thermal conductivity due to rarefied air. The electronics inside these two cameras could freeze or overheat. This is the most likely reason for the failure of these two cameras. As we have already noted, post-flight tests of all the cameras and electronics confirmed full functionality of the SONC imager and no performance degradation. We have provided this information in the revised manuscript (lines 110-117).

line 107: Generally, I suggest to put urls into the bibliography. For this particular one, however, I think it is uncommon to cite news articles in scientific publications. It is safer to remove the link and give the relevant information in the text (to avoid a broken link at some time).
We have replaced this link with a new one which is the most relevant, demonstrating a general description of the TRANSAT flight, its technical characteristics and scientific payload (lines 121-122).

line 109: The infrasound experiment is not used in this study at all, so I suggest to not mention it here.
These two experiments (NLC and infrasound) are combined into the same atmospheric project to investigate wave dynamics at different frequencies and scales. Both of these instruments have a single source of funding. Therefore, we believe that it is appropriate to mention the infrasound experiment in this paper. We keep information on the infrasound experiment mentioned in the manuscript.

line 118: From watching the video, it seems the anti-sun pointing of the gondola was not active during all of the flight. This should be clearly indicated as it likely affects the data analysis.

The anti-sun pointing of the gondola was active most of the time during the TRANSAT flight. Due to different scientific experiments onboard requiring different pointing directions, sometimes the anti-solar direction was not observed, but the rotation of the gondola remained under control. When the Sun illuminated the camera lens or strong solar reflections were present, such images were removed from the analysis as overexposed. Overexposed images do not appear in the keogram and in subsequent analysis. The number of the overexposed removed image accounted for about 2% of the total number of images analyzed. We have provided this information in the revised manuscript (lines 133-137).

Fig. 2: When watching the video, one notices the change in azimuth. I think it would be helpful to plot azimuth as a function of time in addition to height in Figure 2.
We agree with this comment and have added azimuth as a function of time in Fig. 2c.

line 145: In the video, around 2024-06-23 6:02 UTC, there are strong reflections on the camera image. Are these from dust on the camera lens? Was this data removed from the keogram analysis?
Yes, these images and similar ones, having strong reflections from the Sun, were removed from the keogram analysis and successive image analysis as mentioned above.

line 145: There seems to be a vibration (up-down movement of the horizon) at 25 June 8:51 UTC and 26 June 4 UTC. What caused this? Does this effect the keogram analysis?
Sometimes, vibrations of the TRANSAT gondola were caused by strong wind shears in the stratosphere, acting on the auxiliary balloon right above the gondola. This does not affect the keogram analysis because it is based on the relative coordinate system (image frame) and not relative to the ground.

line 145: A white object enters the field of view on 26 June 6 UTC. I am curious what this is?
It was the Moon.

Figure 3: On the image, the structures are hardly visible. It is a bit better in the video. Please add the projected image and the relative brightness from the wavelet analysis to this figure.
We have adjusted brightness and contrast settings in Fig.3a to make the wave structures clearly visible. We have added the projected image in Fig.3c. The relative brightness after subtraction of the background is presented in Fig. 3b. The wavelet analysis (Fig.4) of Fig. 3b shows the power (squared amplitude).

line 146: For how many images was the automatic image processing done? Only one example is shown.
The automatic image processing was applied for ten images, but since statistical analysis is not the purpose of the present study, but only case studies, we limit the presentation of the automatic image processing to only one case.

line 146: More information on the automatic analysis should be given, including plots for each step. Please show the projected image for the example in Fig. 3 and 4. In Figure 4, why is the x-axis labeled with "Pixels along Y-axis of image", when it the text it is stated that the wavelet transform was applied to the projected image? The projected image' dimensions must be latitude/longitude or in units of km, not pixels. Please mark the positions in the original image, where the waves of 30 and 40 km horizontal wavelength were detected. Is it on the top

or the bottom of the original image? Is Figure 4 shown for a single vertical column of the image, or many?

We have provided more information on the automatic analysis in the revised manuscript (lines 170-176). As far as "including plots for each step" is concerned, we skip just one plot for the first step "Background subtraction", which is presented below in Fig. 1. We believe that this plot is superfluous in this case since it does not affect the obtained result. This is because the second step "Two-dimensional digital filtering" successfully removes the background in this case, since there are no strong gradients and trends in the background atmosphere of the analyzed image. Therefore, we do not present this plot in the manuscript, but only in this response to the Reviewer 2. Instead, we have added an example of a 2D-filtered image (with background subtraction) in new Fig. 8 of the revised manuscript, which is more appropriate to demonstrate this step.

Figure 4 was indeed projected onto the Earth's surface, and the scale on the horizontal axis has a dimension in km. At the same time, it is better to consider the position of the analyzed wave packets in the non-transformed original image (Fig. 3a,b) than in the nonlinearly horizontally transformed image (Fig. 3c). The X-axis in pixels more clearly shows the location of the obtained wave maxima on the non-transformed scale in pixels in Fig. 3a,b. That is why we keep the main scale of the X-axis in pixels and have added an additional horizontal scale in km in Fig.4.

The wavelet analysis shown in Fig. 4 is a continuation of the digital filtering of the case study presented in Fig. 3. In Fig. 3c, we have presented the projected image shown in Fig. 3a. We have marked the vertical column where the waves of 30 and 40 km horizontal wavelengths were detected in Fig. 3a and 3b. Figure 4 is shown for the single vertical column with X=2200 pixels as shown in Fig. 3a and 3b. We have added this information in the revised manuscript (lines 180-184).

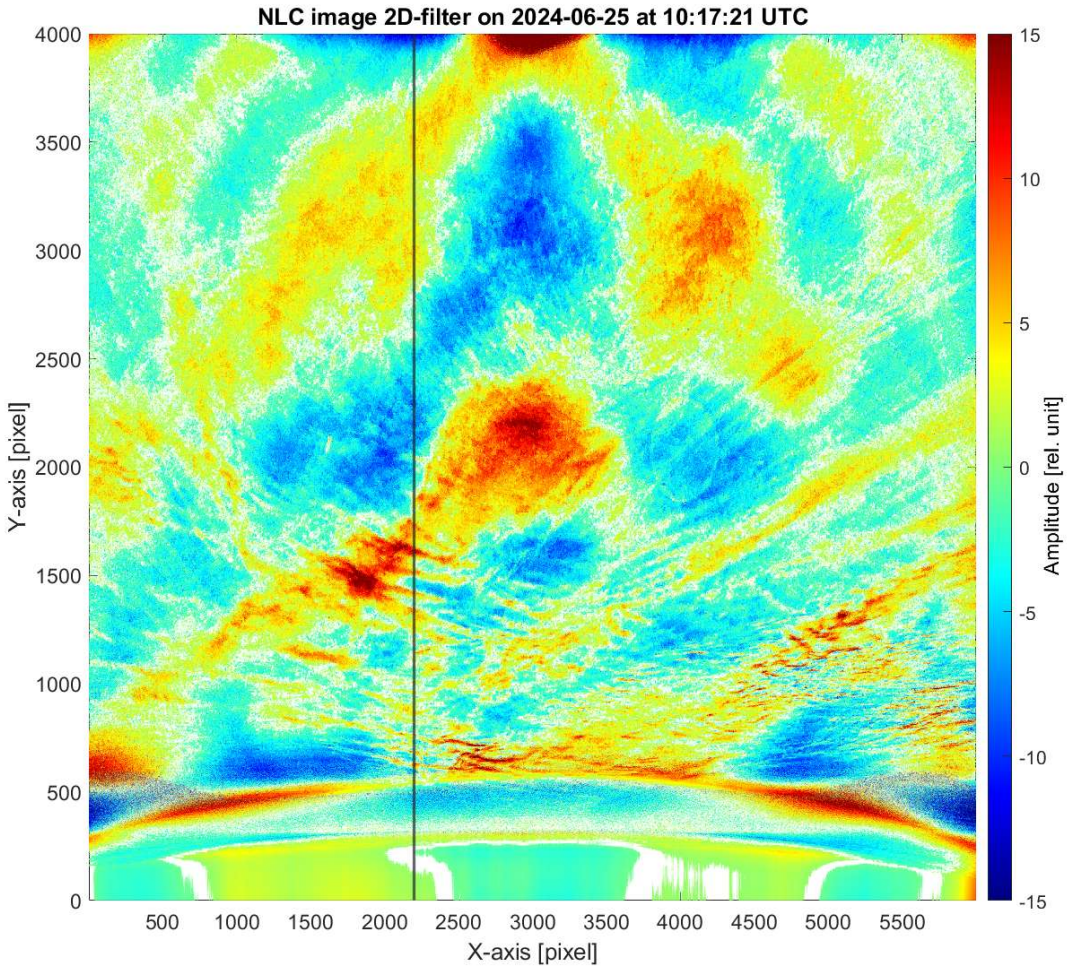

Figure 1. This is step 1 in the automatic analysis of NLC images obtained from the stratosphere, demonstrating the background subtraction: a second-order polynomial fit was used to estimate the sky background along each vertical and horizontal line in the image, which was then subtracted to yield a residual brightness of each pixel. Not for publication.

line 170: "at which NLC preferred to appear" Could it be that the sensitivity of the camera or the viewing geometry is most favourable in this part of the image? Close to the horizon, the camera observes the NLC layer at a lower angle compared to the top of the image closer to zenith. Please state at which distance from the gondola positions these pixel positions are. These must be farthest away, maybe a 1000 km?

Here one can talk about the influence of relative and absolute effects. The relative effect is that the optical depth of the NLC layer increases at lower angles in comparison with angles close to the zenith. On the other hand, the atmospheric background becomes brighter at low elevation angles and very bright near the troposphere. Therefore, this range of pixels in the images is optimal. In addition, there is the absolute effect. NLC form more often towards the horizon in the northern part of the sky, since the temperature in the mesopause decreases at high latitudes compared to middle and low latitudes. Therefore, when the camera is pointed to northwest-north-northeast, there is a greater chance of detecting NLC at lower elevation angles, as they are visible farther north of the mesopause with lower temperatures.

These pixels (3000-3400) correspond to a distance of about 315-580 km from the gondola position. We have added this information in the revised manuscript (lines 214-215).

line 171: Is the keogram constructed from projected or unprojected images? Fig. 3b, where we can see pixels 3000-3400, is unprojected, but then it makes no sense that (l. 151) "each image was projected prior to the analysis" in this (1)-(4) sequence of steps.
The keogram was constructed from unprojected images. Image projection was applied to wavelet analysis only. We have made it clearer in the revised manuscript (line 178).

line 177: Does "the manual procedure" refer to the video? It is stated in line 141 that the images in the video were marked for NLC presence or absence, but no results are shown. Can this be added to Fig. 5?
The manual procedure applies to all analyzed 6200 images without compression. They are of higher quality, since the video procedure uses compression of all images. In the manual procedure, a separate text file was created that indicates the cloud-free times. These times coincide with the times obtained in the automatic procedure, as indicated in Fig. 5. Therefore, the addition of cloud-free times made in the manual procedure does not provide any additional information in this case. We have provided this information in the revised manuscript (lines 163-164, 224-225).

line 174: Is one standard deviation enough? Did you check other values, does the result change? Is the mean brightness (and sensitivity of the camera to NLC) constant for all times? Does it depend on the azimuth, or its deviation from anti-sun?
Yes, one standard deviation is enough. During a pre-analysis we checked others values, which produced a similar result.
The mean brightness and standard deviation differ for different images. Therefore, we separately estimated the mean brightness and standard deviation for each image. The sensitivity of the camera to NLC is a relative quantity that can be defined in different ways. Importantly, we estimated the mean brightness and standard deviation for each image, thus the obtained values are independent of time.

The keogram is independent on the azimuth as the mean brightness and standard deviation are determined for each image. The exception is strong reflections coming from the Sun. But we excluded such images from the analysis as described above.
We have provided the relevant information in the revised manuscript (lines 218-219).

Figure 5. It is worth noting that the times in the caption do not correspond to the times of the gondola position shown in Fig. 2a because it shows NLC observed at a long distance (the NLC position depending on azimuth).
The UTC times shown in Fig. 5 do correspond to the UTC times shown in Fig. 2a. The corresponding LSTs shown in Fig. 5 have been calculated for the position of the gondola. The Reviewer 2 is right that the LSTs do not refer to the observed NLC, because NLC were observed at a distance of about 300-600 km from the gondola, and the LST for NLC does depend on the viewing azimuth. We have added this information to the caption of Figure 5.

Fig. 5: Please add the number of y-pixels for which this keogram was constructed to the caption.
We have added this information to the caption of Figure 5.

Fig. 5: I think during the first 12 h the effect from the unstabilized gondola is seen as vertical stripes. The keogram can only be interpreted knowing the azimuth.
The Reviewer 2 is right that the periodic vertical stripes (mainly bright wave crests) in the first 12 hours of the flight are caused by periodic oscillations of the gondola around the leading azimuth (Fig. 1c). These azimuth oscillations were planned and were under control. However, this does not negate the obtained result which is aimed at detecting the presence of NLC at a given time and space. The exact spatial location of the observed NLC cannot be directly represented on the keogram. To do this, it is necessary to combine the keogram with the position of the gondola and with the orientation of the camera (Fig. 1a, c). However, calculating the exact position of all observed NLC is beyond the scope of this analysis, excepting three NLC cases presented in Sections 3.2, 4.2 and 4.3.

line 195: It is not of relevance for this paper that the ALOMAR lidar can measure polar stratospheric clouds in winter, or stratospheric aerosols. Please only state necessary information. For example, temperature and winds would be useful for interpretation of the NLC layer shown in Fig. 6. But as these are not shown, it can be removed.
In the paper by Hildebrand et al. (2017), https://doi.org/10.5194/acp-17-13345-2017, it was mentioned that "The ALOMAR RMR lidar (69.3°N, 16.0°E) is a twin lidar with two identical transmitting lasers, two identical receiving telescopes and one detection system. It measures temperatures and aerosols in the middle atmosphere on a routine basis since 1997 (von Zahn et al., 2000; Schöch et al., 2008)", although only temperature and horizontal wind measurements were analyzed between 30–85 km altitude in the paper.

In the paper by Strelnikova, et al. (2021), https://doi.org/10.1175/JAS-D-20-0247.1, it was mentioned that "the lidar provides observations of temperatures, winds, aerosols, and noctilucent clouds during day- and nighttime (e.g., von Zahn et al. 2000; Schöch et al. 2008; Fiedler et al. 2011; Baumgarten et al. 2015)", although only temperature measurements from 30 to 70 km were analyzed in that paper.

In the paper by Mossad et al. (2025), https://doi.org/10.5194/egusphere-2025-3267, it was mentioned that "The Doppler Rayleigh-Mie-Raman (DRMR) lidar in the Arctic Lidar Observatory for Middle Atmosphere Research (ALOMAR) located in northern Norway (69°N, 16°E), has been measuring atmospheric temperature, stratospheric aerosols, mesospheric ice particles and horizontal wind velocities for 30 years so far (von Zahn et al., 2000; Fiedler and Baumgarten, 2024).", although only temperature and horizontal wind measurements were analyzed between 35–60 km altitude in the present study.

In other words, it is common practice to give a brief description of the instrument and its principal capabilities for measuring atmospheric parameters. This is useful for educational purposes, especially for young scientists and for scientists in interdisciplinary fields of knowledge, who have not read the basic papers on this instrument. Therefore, we retain this basic information about the instrument in the present manuscript.

Figure 6: Can the lidar measurements be shown with the same quantity for color? It is very hard to compare "RayHi backscatter signal in Hz" to backscatter coefficients. It seems when the Esrange raw counts would be converted to backscatter coefficients, it might not be significant at this high resolution. Maybe it would be better to bin Esrange data to 1 km x 1 h?

The procedure of converting the Esrange raw counts to the backscatter coefficient is not trivial and beyond the scope of the present study. It is possible to compare the ALOMAR and Esrange lidars measurements in terms of height-time variations. In Fig. 6, we have added a new panel C, demonstrating filtered Esrange lidar data, thus highlighting the basic height-time variations of the NLC layer seen between 20 and 01 UTC. We have provided relevant information in the revised manuscript (lines 251-256).

line 206: It is not "clearly seen in both lidar measurements". There is an enhancement of signal at 3 UTC over the whole column 80-87 km at Esrange, which is very different from ALOMAR. It is hard to see from the plot if all is noise or what part is significant.
Here we mean that NLC signals were clearly see in both lidar measurements from 20:30 until 01:00 UTC. We have already mentioned in the manuscript that "*After 01 UTC, Esrange lidar measurements become too noisy to distinguish the NLC signal from noise*." We do not discuss an NLC layer in the Esrange lidar data after 01 UTC on 23 June. In Fig. 6, we have added a new panel C, demonstrating the filtered Esrange lidar data, thus highlighting the basic height-time variations of the NLC layer seen between 20 and 01 UTC.

Fig. 6: Can you add a projected SONC image when the two stations are in the field of view of the imagers? Unluckily, I suppose, at 7 UTC, when the NLC brightness at ALOMAR increases, the imagers looked west, away from ALOMAR?
We have checked this geometry. The Reviewer 2 is right. When the two lidars observed NLC, the camera was facing the east-south-west part of the sky, and the stations were not visible in the field of view of the SONC imager. The favorable geometry of NLC observations over the ALOMAR lidar appeared at 09:34 UTC on 23 June. We have added a new Figure 7 in the revised manuscript which shows the image with NLC above the ALOMAR lidar at the end of the lidar NLC observation.

line 210: "turbulent vorticities": the phrasing is uncommon. Maybe "instabilities"? Turbulence is not visible at these scales, I think.
We have removed "turbulent vorticities" from the manuscript here.

line 217: "nearly the same NLC" please add SONC images to prove this
In the revised manuscript, we have added a new Figure 7 which illustrates the SONC images at 22:04:38 UTC on 22 June and at 09:34:32 UTC on 23 June, i.e., at the beginning and end of NLC observations by the Esrange and ALOMAR lidars. At the beginning of the lidars measurements the NLC observed by the SONC imager were located to the east of the lidars, but at the same latitude range (Fig. 7a). Later, the SONC imager slowly rotated in the antisolar direction, observing the east-south-west sector of the sky, and, thus, observations of NLC in the mesopause over the lidars were impossible. At the same time, at the very end of the ALOMAR lidar NLC observations at about 09:30 UTC on 23 June, the SONC imager looked north-northeast and detected faint NLC at the very edge of the image frame directly over the ALOMAR lidar (Fig. 7b). At that time, NLC were between 81.5 and 82.5 km. We have added this information in the revised manuscript (lines 278-286).

line 219: What is the scientific conclusions from the presented measurements?
Lidar measurements complement balloon-borne observations, providing information on vertical dynamics of the NLC horizontal layer observed from the stratosphere.

line 247: A discussion of the resolution of the SONC image data should be added to this work. From Fig. 3a and the video, it can be doubted that "smaller gravity waves and turbulent structures" can be detected. As the images were projected, please include an assessment of the largest and smallest scales that can be observed.
We have included an assessment of the largest and smallest scales that can be observed in the revised manuscript (lines 185-193).

line 250: "complement each other". In line 231, it was stated that MATS provides high-resolution images and three-dimensional fields of NLC properties. Is Fig. 7b the high-resolution image? As the satellite likely passes several times per day, was this the only coincidence?
The spatial resolution of Fig. 7b (new Fig. 8c) is 5.7 km × 290 m. The horizontal resolution of 5.7 km is on par with AIM/CIPS data and the vertical resolution of 290 m should be considered high for satellite missions. We have added this information in the revised manuscript (lines 303-305).

As the Reviewer 2 correctly noted, in the next orbit, MATS again registered NLC over Greenland and in the field of view of the SONC imager, which is shown in Figure 2 below (not for publication). The purpose of this study is not to completely compare all possible NLC observations from the stratosphere and the satellite, but to demonstrate the fundamental possibility of such observations in one figure only. We have added the relevant information in the revised manuscript (lines 319-323).

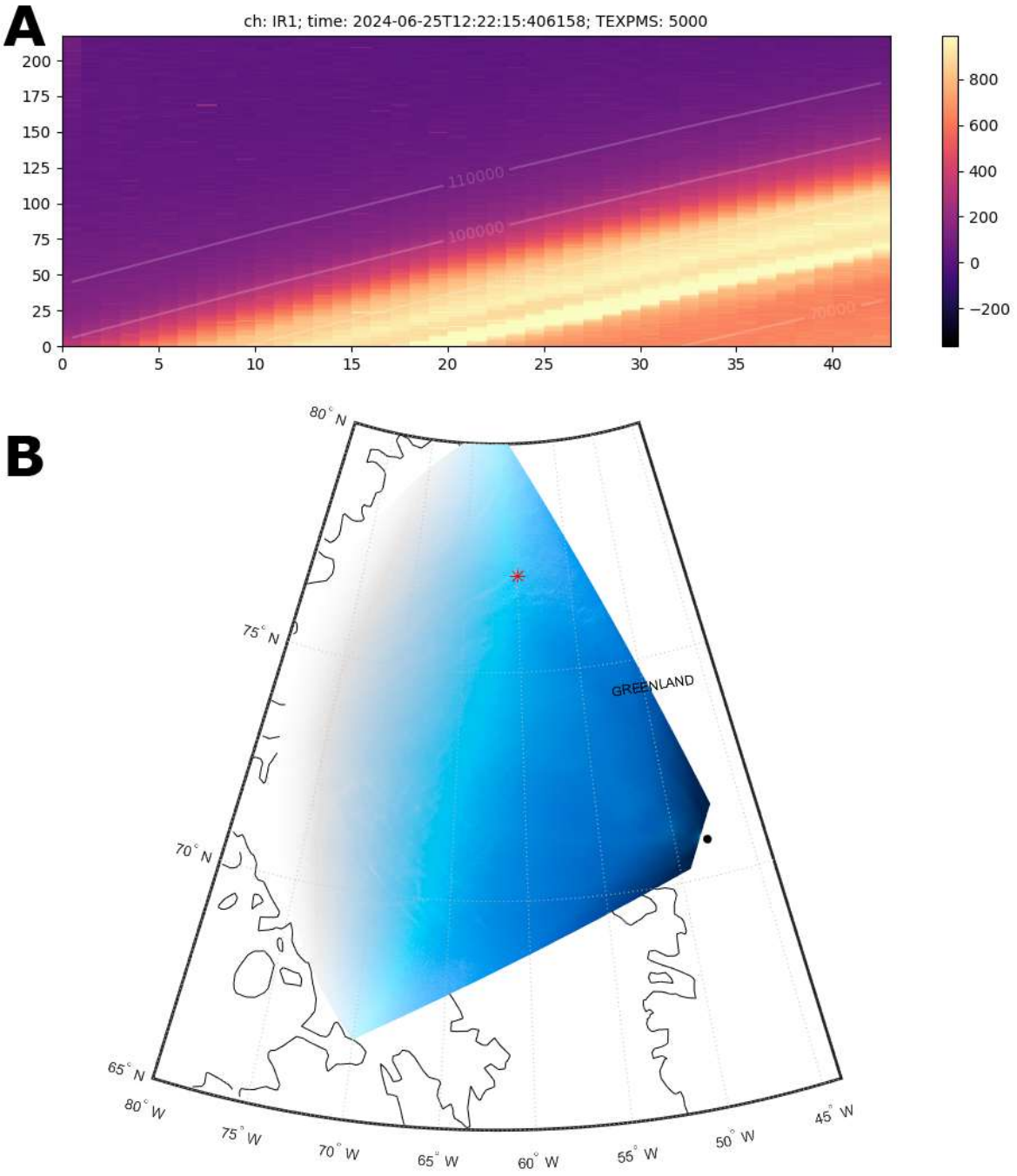

Figure 2. Example of NLC measurements obtained from the stratosphere and space on 25 June 2024 during the TRANSAT balloon flight. (A) Image, taken by the MATS satellite at 12:22:16 UTC, illustrate part of the atmospheric limb, with the bright yellow PMC layer seen between 80 and 85 km. Data are shown for the IR channel 1 at 762 nm. (B) Projection of an NLC image, taken by the SONC imager, from the stratosphere at 12:22:12 UTC. The black dot is the position of the TRANSAT balloon, the red asterisk marks the MATS tangent point which is in the field of view of the SONC imager (not for publication).

Fig. 7a: As a second-order polynomial was removed in the analysis, would it be useful to show this image also, in order to see the structures more clearly? The original image printed out hardly shows structure.

A 2D-filtered image, removing a second-order polynomial, has been added in new Figure 8 (lines 325-327).

line 263: Why is it unexpected? There is a long history of AIM imagery of NLC. What is expected from the AIM climatology for this time of year and location? E.g. in 2022, AIM shows strong and widespread NLC https://lasp.colorado.edu/aim/browse-images

NLC activity is highly dependent on geographic latitude. This is well known from many previous NLC observations and is also clearly visible in AIM/CIPS images. The SONC camera observed NLC in the latitudinal range of 60-75 degrees north, depending on the azimuth of the camera's pointing. If one look closely at AIM/CIPS images at the end of June of any year of available measurements, one can clearly see gaps in NLC at these latitudes of at least from 60 to 70 degrees north. It is seen both on an individual "daily daisy" composite images and on a series of such images for several days. That is, NLC were not observed continuously at these latitudes. In addition, AIM had a sun-synchronous orbit, taking measurements only twice a day at a given longitude. That is, AIM measurements cannot be used to study NLC diurnal variations in detail. This can be done either with the help of continuous lidar measurements or with the help of stratospheric flights for several days.

Indeed, continuous lidar measurements of NLC at high latitudes (at latitude of 69°N) show that the maximum NLC occurrence frequency is about 65% in the morning hours and drops to about 35% around noon. That is, there are clear solar diurnal and semi diurnal variations (see Fig. 4 in Fiedler et al., 2011). We have added this information in the revised manuscript (lines 346-347, 361-364).

Thus, it is impossible to talk about continuous NLC observations at latitudes of 60-70°N at least. The discontinuity of NLC observations was also confirmed by the previous NLC observations from the stratosphere during the PMC Turbo balloon flight from Sweden to Canada in July 2018, which we have already mentioned in the manuscript. Therefore, almost continuous observations of NLC during the TRANSAT flight is an unexpected scientific result.

line 265: Please add mean latitude and longitude of these time periods, as they do not relate to the gondola positions shown on the map.

We have added the positions of these four intervals of NLC disappearances as shown by the blue circles in Fig. 2a.

line 291: The third interval on the 25th is the longest. Does JAWARA show similar temperature enhancements for this time and location?

At about 84 km altitude, between 18 and 22 UTC on 25 June, JAWARA temperatures were below 147 K (supposed to be a temperature threshold for NLC from previous studies), which generally allow the existence of ice particles in the observed region of the mesopause. After 22 UTC on 25 June and until 03 UTC on 26 June, JAWARA temperatures were above 147 K, thus prohibiting the existence of ice particles. Thus, JAWARA temperatures can explain the NLC disappearance after 22 UTC, but not before that time. At the same time, it is well known from previous studies (i.e., Rong et al., 2012, https://doi.org/10.1029/2011JD016464; Pertsev et al., 2014, https://doi.org/10.1186/1880-5981-66-98; Hervig et al., 2015, https://doi.org/10.1016/j.jastp.2015.07.010) that not only temperature, but also the amount of water vapor plays a significant role in the formation of ice particles. In a

given space and time of the mesopause, there could be a small amount of water vapor, insufficient for the formation and existence of ice particles.

On the other hand, at about 81 km altitude, JAWARA temperatures were above 147 K already after 17 UTC on 25 June, which did not allow the existence of ice particles. It is possible that the NLC layer was simply at the bottom of the mesopause region at that time where temperatures were too high for NLC to exist, as, for example, the ALOMAR lidar measurements demonstrated at the end of the NLC measurements on 23 June (Fig. 6a).

Therefore, one cannot expect a 100% agreement between JAWARA temperatures and the observed NLC activity. In some cases, there is good agreement, as the two NLC cases demonstrated in this paper, in other cases there may not be such good agreement.

line 371: Was the estimation of speeds performed on projected images? Can a sequence of two projected, background-removed image be shown that highlights speed and directions of the two layers?
Yes, the estimation of NLC velocities (speeds and directions) was performed on projected images. It is possible to use a sequence of two projected background-removed images, but this technique has no advantages and even has disadvantages compared to the analysis of original images by the following reasons:
1. Projected images, as stated above, produce a non-linear horizontal transformation of all pixels in image. We use a manual procedure to trace small points in NLC. It is more difficult to trace the analyzed small points in NLC when using projected images.
2. Relative brightness of the analyzed NLC points changes after subtraction of the atmospheric background since different background brightness is estimated on two images, and subtracting two different backgrounds (along both horizontal and vertical lines) produces different relative brightnesses of the analyzed traced NLC points, which are more difficult to compare.

That is why the trace analysis of NLC points was applied to the original (unfiltered and unprojected) images. After completing the trace analysis, the estimation of NLC velocities (speeds and directions) was performed on projected images as stated above. We have added this information in the revised manuscript (lines 461-463).

line 449: It is not "unprecented", as there was previous imaging from stratospheric balloons
This formulation “unprecedented view of mesospheric cloud dynamics” refers to a general advantage of NLC observations from the stratosphere compared to ground-based and satellite platforms. We have corrected this sentence to make it clearer in the revised manuscript (line 542).

line 453: Why were only 6200 images from 40'000 images used? As the 6200 cover all times, were all the other images taken in between? Had they unsuitable exposures such that they could not be used, or what is the reason for excluding so many images?
The other images taken in between did indeed have unsuitable exposures (either overexposed or underexposed). In the present paper, we used one image from a series of 5 images that are suitable for automatic image processing. However, this does not mean that other images cannot be used in further studies for special cases, using a more sophisticated image processing technique. For example, we did analyze some images

which have strong reflections from the Sun, but it required not standard algorithms of image processing. This is beyond the scope of the present study.

line 472: Is point 5 based on a single image only? As the automatic analysis is not used to obtain statistics in this work, it should be motivated why it was done. Is it to determine the smallest observable scales?
Yes, point 5 is based on a single image only. This example was chosen at random from 6200 images, but which demonstrates the NLC modulation due to gravity waves with the naked eye. Therefore, we were interested in applying this image analysis technique to this image in order to estimate the horizontal scales of the wave packet in this case. We have added this information in the revised manuscript (lines 182-184).

line 474: The result that NLC disappearance was linked to a warming is consistent, but not surprising, as the dependence of NLC occurrence on ambient temperature is known. Section 4.2 lacks citations of previous work on this topic.
This result is not just about a warming of the mesopause (it is indeed well-known), but it is mainly about the intrusion of a warm air mass from middle to high latitudes. During analysis of this case, in the beginning, it was supposed that it could be a large-scale mountain gravity wave coming from the Greenland mountain range. The ERA 5 assimilation model was analyzed for this specific case to investigate a potential presence of a mountain wave from 0 to 80 km. However, the ERA 5 analysis did not reveal a presence of a mountain wave in the troposphere, stratosphere and mesosphere in the space-time domain analyzed. Then the JAWARA model was analyzed that revealed the presence of the warm spot in this specific space-time domain in the mesopause region, that was connected to the air mass intrusion from middle latitudes. However, it is not a trivial case to obtain such a result since it requires knowledge on temperature and wind velocity at specific time and space in the mesopause region. This is a very rare case study when such information about the mesopause environment is available and published.

Spelling and grammar
line 161: obtaned -> obtained
it has been corrected.

line 165: Language of this paragraph should be improved, e.g. "Keogram is a slice.." -> "A keogram is a a slice..", singular, plural etc.
Language has been corrected in this paragraph.

line 198: "during the TRANSAT flight in the stratosphere" please remove "in the stratosphere"
It has been removed from the revised manuscript.

line 215, line 238: "from the stratosphere" -> "by the SONC imager" or "from the TRANSAT balloon"
It has been corrected.

line 216: "lunch" -> "launch"
It has been corrected.

line 228: "6" -> "six"
It has been corrected.

line 254: Delete "from the stratosphere"
It has been deleted.

line 354: TRANSAN -> TRANSAT
It has been corrected.